Decay of $_{60}Nd_{89}^{149}$

R. G. HELMER AND L. D. MCISAAC
Phillips Petroleum Company, Atomic Energy Division, National Reactor Testing Station, Idaho Falls, Idaho

(Received 11 October 1965)

The level structure of $_{61}Pm_{88}^{149}$ has been studied from the decay of 1.7-h Nd^{149}. Studies were made of the internal-conversion electron spectrum with magnetic spectrographs, and of the gamma-ray spectrum with NaI(Tl) and Ge(Li) detectors. Gamma-gamma coincidence experiments were carried out with NaI(Tl) and Ge(Li) detectors. Beta-gamma coincidence measurements were made with combinations of proportional counters and anthracene, NaI(Tl), and Ge(Li) detectors. The half-life of Nd^{149} was found to be (1.73±0.01) h. About seventy gamma-ray transitions from 30 to 1456 keV were observed. The transitions with intensities greater than 1% of the decays have the following energies, transition intensities, and multipolarities: 30.0 (~6%, *E*2), 59.0 (~2), 74.4 (~2), 97.0 (~3, *M*1), 114.3 (38, *M*1), 155.9 (6.2, *E*1), 188.8 (2.0), 198.9 (1.4), 208.2 (2.6), 211.3 (24, *M*1), 240.3 (6.5, *M*2), 267.7 (7), 270.3 (10, *E*1), 326.6 (4.5), 349.1 (1.5), 423.6 (7), 443.5 (1.1), 540.5 (6.5), 556.4 (1.1), and 654.7 (8.4). The 240-keV transition has a half-life of 41 μsec which agrees with the *M*2 assignment based on the internal-conversion coefficients. From previous lifetime measurements for states at 114 and 270 keV, hindrance factors were computed for the following gamma-ray transitions: 114 keV (*M*1, 350), 270 keV (*E*1, ~5×10⁵), 155 keV (*E*1, ~5×10⁵), and 59 keV (*E*1, ~5×10⁴). The 30-keV transition between the 270- and 240-keV levels appears to be enhanced by a factor of about 80. A level scheme is proposed which includes about sixty transitions. There are well-established excited states at 114.3, 188.8, 211.4, 240.3, 270.2, 387.6, 538.0, 654.8, and 768 keV.

INTRODUCTION

THE nucleus Nd^{149} can be produced by neutron capture in stable Nd^{148} or as a fission product. It decays with a 1.7-h half-life by beta emission to $_{61}Pm^{149}$ which in turn decays with a 53-h half-life to stable Sm^{149}.

A transition from nuclei with stable spherical shapes to nuclei with spheroidal deformation in the ground states appears to take place between neutron numbers 88 and 90. Therefore, the states in Pm_{88}^{149} and the decay from Nd_{89}^{149} may be of interest in regard to the information they give about this transition.

The first extensive study of the decay of Nd^{149} was the internal-conversion-electron work of Rutledge *et al.*[1] Recent studies, primarily by means of scintillation spectrometry, have been reported by Gopinathan and Joshi,[2] Chen and Arns,[3] and Nieschmidt *et al.*[4] A report by Rider *et al.*[5] includes scintillation studies and extensive Nd^{149} half-life determinations. A series of measurements of lifetimes of levels in Pm^{149} have been reported by Currie and Dougan[6] and two measurements have been reported by Fossan *et al.*[7] These studies report from 14 to 22 gamma rays whose energies are all below 700 keV.

EXPERIMENTAL METHODS

Several types of experimental measurements were made in order to determine the properties of the gamma-ray transitions in the decay of Nd^{149}. The methods used in the collection and analysis of the experimental data are summarized.

Gamma Rays

Gamma-ray spectra were measured with a 3 in.×3 in. NaI(Tl) scintillation detector and a multichannel analyzer. The response of this system to monoenergetic gamma rays has been studied in detail.[8] As a result, it is possible to calculate the spectral distribution for a gamma ray of any desired energy between 0.1 and 2.1 MeV. These calculated gamma-ray shapes were used along with estimated bremsstrahlung shapes as input to a least-squares fitting program in order to obtain the relative gamma-ray intensities. Details of this analysis are given in the Appendix.

Gamma-ray spectra were also determined with lithium-drifted germanium detectors of 2 and 4 mm thickness. These spectra were used to obtain transition energies and relative intensities of gamma rays that are not resolved in data taken with NaI scintillation spectrometers. The peak positions were determined by fitting the points in the peak with a Gaussian function. These positions were then corrected for the measured nonlinearity of the electronic system. Then the energies were determined from a linear function through two calibration points. The gamma-ray intensities were computed by the methods described in the Appendix.

† Work performed under the auspices of the U. S. Atomic Energy Commission.

[1] W. C. Rutledge, J. M. Cork, and S. B. Burson, Phys. Rev. **86**, 775 (1952).

[2] K. P. Gopinathan and M. C. Joshi, Phys. Rev. **134**, B297 (1964).

[3] C. H. Chen and R. G. Arns, Nucl. Phys. **63**, 233 (1965).

[4] E. B. Nieschmidt, V. R. Potnis, L. D. Ellsworth, and C. E. Mandeville, Bull. Am. Phys. Soc. **10**, 442 (1965).

[5] B. F. Rider, J. P. Peterson, Jr., C. P. Ruiz, and F. R. Smith, U. S. Atomic Energy Commission Report GEAP-4621, 1964 (unpublished).

[6] W. M. Currie and P. W. Dougan, Nucl. Phys. **61**, 561 (1965).

[7] D. B. Fossan, L. F. Chase, Jr., and K. L. Coop, Phys. Rev. **140**, B1 (1965).

[8] R. L. Heath, R. G. Helmer, L. A. Schmittroth, and G. A. Cazier, U. S. Atomic Energy Commission Report IDO-17017, 1965 (unpublished).

4π β-γ Coincidence System

A 4π β-γ coincidence system was used to determine the constant by which one converted the relative gamma-ray intensities into absolute intensities. The system consists of a gas-flow electron counter with the source mounted on a thin backing (~ 10 $\mu g/cm^2$, gold-coated, VYNS film) at the center of the detector. A 3 in.$\times$3 in. NaI(Tl) crystal is mounted outside the electron counter.

The disintegration rate of a particular source was determined from the total singles and coincidence counting rates.[9] Then a gamma-ray spectrum was obtained for the same source in a known geometrical arrangement in order to determine the absolute intensity of one or more gamma rays.

Conversion Electrons

Internal-conversion electrons were observed photographically in a set of 180°, permanent-magnet spectrographs. (Several dozen plates were made with various exposures and with sources which had decayed for various times.) The sources were made from neodymium oxide enriched to $\sim 90\%$ in Nd^{148}. This material was vacuum evaporated from a tantalum filament onto graphite blanks. Typical sources were $1\frac{1}{2}$ cm$\times$0.025 cm in area. The complete blanks were then irradiated in a flux of 2×10^{14} neutrons cm^{-2} sec^{-1}. The Nd^{149} sources were usually placed in the spectrographs thirty minutes after the irradiation. This allowed the 12-min Nd^{151} to decay sufficiently to be unobserved. Plates exposed after the decay of the Nd^{149} indicated the presence of Pm^{149} and in some cases Ta^{182} and Ta^{183} from the filament.

One can easily distinguish the lines of Nd^{149} from those of Nd^{151}, Nd^{147}, Pm^{147}, Pm^{149}, and Pm^{151} by their half-life. To insure that there was no impurity with a half-life of a few hours, the following experiment was performed. A sample was irradiated, non-rare-earth elements were removed, and the rare earths were separated by use of an ion-exchange column. The neodymium fraction was plated onto a 0.006 in. diam platinum wire which was used as a spectrograph source. This source was not intense enough to observe the weakest lines (e.g., K-424), but all the other lines were verified as being from Nd^{149}.

The spectrographs have been previously calibrated[10] and energy measurements are believed to be accurate, without internal calibration, to 0.1% or 0.1 keV, whichever is larger. This calibration was improved somewhat by use of two internally calibrated sources. These consisted of $Nd^{149}+Ta^{182}+Ta^{183}$ and $Nd^{149}+Ir^{192}$. The Nd and Ta or Nd and Ir were evaporated at the same time and thus the source positions were identical. This eliminated any systematic error in the calibration.

The relative intensities of the conversion lines were determined from the spectrograph plates. For these measurements a set of plates was exposed sucessively with the same source. For this set of plates, it was assumed[11] that

$$\log_{10}(I_0/I)=C\log_{10}(\alpha E+1),$$

where E is the exposure (in electrons cm^{-2} or proportional units), I_0 is the light intensity transmitted through an unexposed portion of plate, I is light intensity at any exposed portion, α is a scaling factor which can be taken as unity, and C is a constant to be determined. The quantity $\log_{10}(I_0/I)$ is the optical density, and it was determined by scanning the lines with a microphotometer. From the half-life of the source and the exposure times, the relative values of E for a line can be computed for a set of plates. (The ratio is the same for all the lines on this set of plates.) The value of C which best fits the calculated ratios of E and the measured $\log_{10}(I_0/I)$ values was computed for each of several lines. The average value of C was then used to compute the relative exposures for each line. The relative intensities were calculated by use of the average relative exposures, the "rectangular approximation" of Ref. 11, and an empirical curve for the emulsion sensitivity, ϵ. This method gives reasonable intensities for the lines from sources of Ta^{182} and Ir^{192}. In the most favorable cases the relative line intensities should be accurate to about 10%, while most ratios should be accurate to 20%.

The relative intensities of some of the conversion lines were also determined from a spectrum from a silicon surface-barrier detector. For electron energies as measured here, the detector is operated at a bias such that electrons below 400 keV will be stopped in the sensitive volume. This reduces the gamma-ray detection efficiency from that for higher biases. In analyzing these spectra it was assumed that for lines of equal intensity, the peak areas are the same, independent of the line energy.

γ-γ and β-γ Coincidence Experiments

Gamma-gamma coincidence measurements were carried out with either two NaI(Tl) crystals or with one NaI(Tl) detector and one lithium-drifted germanium detector. The germanium detector was 2 mm thick and had a resolution of about 7 keV. The linear amplifiers provided a double-differentiated output signal. The "crossover" point of this pulse was used to provide the fast-coincidence timing pulse. Commercial coincidence circuits were used; they were operated with a resolving time, 2τ, of 0.1 μsec.

For coincidence events, the amplitudes of the pulses from both detectors were determined in a two-parameter analyzer. The events were then either stored in a 4096-

[9] See, for example, R. A. Allen, in *Alpha-, Beta-, and Gamma-Ray Spectroscopy*, edited by Kai Siegbahn (North-Holland Publishing Company, Amsterdam, 1965), Vol. 1, Chap. VII, p. 443.

[10] R. G. Helmer, U. S. Atomic Energy Commission Report IDO-17042, p. 44, 1964 (unpublished).

[11] H. Slätis, Arkiv Fys. **22**, 517 (1962).

TABLE I. Gamma energies (in keV) from Nd+Ir plates.

Ir^{192} lines				Nd lines			
Line energy	Assignment	E_γ	Best values	Line energy	Assignment	E_γ	Average
58.05	K -Pt	136.43		51.78	K	96.98	97.0
123.07	L_2 -Pt	136.33					
124.69	L_3 -Pt	136.24		68.99	K	114.19	
	average	136.33	136.34±0.02[a]	106.93	L_1	114.36	114.3
131.95	K -Os	205.85		166.00	K	211.20	211.2
193.44	L_2 -Os	205.82					
194.85	L_3 -Os	205.71					
203.51	M_3-Os	205.96					
	average	205.84	205.79±0.02[a]				
217.60	K -Pt	295.98					
282.58	L_2 -Pt	295.84					
284.64	L_3 -Pt	296.19					
	average	296.00	295.93±0.03[b]				
230.05	K -Pt	308.43					
295.29	L_2 -Pt	308.55					
	average	308.49	308.46±0.03[b]				
238.18	K -Pt	316.54					
303.11	L_2 -Pt	316.37					
304.91	L_3 -Pt	316.46					
	average	316.46	316.50±0.03[b]				
389.84	K -Pt	468.22	468.0 ±0.1[b]				

[a] Value from Ref. 12.
[b] Average of values from Refs. 12 and 13.

channel, magnetic-core memory or on a magnetic tape which provided 256×256 channels. In the former case, the portions of the spectra to be stored in the memory are selected by a set of digital gates. For example, one can store 32 spectra each 128 channels long with the 32 channels representing the third group of 32 channels (i.e., 64–95) from one analyzer and the 128 channels spanning the second half of the other 256 channel ramp. In the second case, all coincidence events are stored on the magnetic tape which is processed by a computer to provide 256 spectra each 256 channels in length. For the purpose of analysis, various numbers of spectra with adjacent "gates" can be added together to provide better counting statistics in regions where narrow gate widths are not necessary.

The coincidence spectra were interpreted both by visual analysis of the resulting plots and by computer fits to selected spectra. In the latter case, the coincidence spectra were "gain-shifted" to a standard gain scale (i.e., 5 or 10 keV per channel). Then the required gamma-ray shapes were computed[8] and the spectra fitted. Bremsstrahlung components and random coincidence spectra were included in the fits. See the Appendix for examples.

When the germanium detector was used it was taken as the gating channel and the NaI(Tl) spectra were displayed and analyzed.

For β-γ coincidence measurements, an anthracene detector was used for the beta rays and a germanium detector for the gamma rays. The beta spectra were displayed.

Nd^{149} samples were used for a period up to about 6 h after the irradiation. During this period the activity of the source was kept constant to within 30% of the average counting rate. These samples were not chemically purified.

PROPERTIES OF TRANSITIONS

Energies and Interpretation of Internal-Conversion Electrons

The electron-line energies and transition energies for a source of Nd^{149} together with Ir^{192} are given[12–14] in Table I and those for a source of Nd^{149} with Ta^{182} and Ta^{183} are given in Table II. For the iridium, the average transition energies agree with the "best" reported values to within 1 part in 3000 and there is no systematic difference. The tantalum transition energies in Table II are systematically lower than the best values by about 0.04 keV. (This would correspond to a combined error of only 0.004 cm in the source position and in the location of a reference notch on the plates.) This slight systematic error was considered in averaging these Nd^{149} energies with those in Table I. It is assumed that

[12] B. Lindström and I. Marklund, Nucl. Phys. **49**, 609 (1963).
[13] G. Murray, R. L. Graham, and J. S. Geiger, Nucl. Phys. **63**, 353 (1965).
[14] J. J. Murray, F. Boehm, P. Marmier, and J. W. M. DuMond, Phys. Rev. **97**, 1007 (1955).

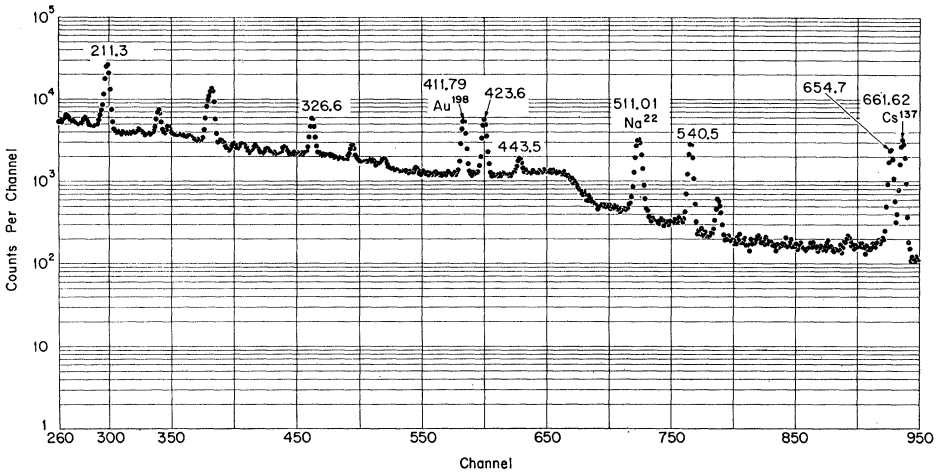

FIG. 1. Gamma-ray spectrum of Nd^{149} along with Au^{198}, Na^{22}, and Cs^{137} obtained with lithium-drifted germanium detector. Lead and tantalum absorbers were used to attenuate the radiations below 200 keV. Energies are in keV. The germanium detector was 4 mm thick and had a resolution of 2.8 keV.

TABLE II. Gamma energies (in keV) from Nd^{149}+Ta^{182}+Ta^{183} plates.

Ta^{182}				Nd^{149}			
Line energy	Assignment	E_γ	Crystal-spectrometer values (Ref. 14)	Line energy	Assignment	E_γ	Average
15.07	K	84.58		22.94	L_2	29.96	
74.47	L_3	84.67		23.55	L_3	30.01	
	average	84.62	84.67±0.02	28.53	M_3	29.89	30.0
53.57	L_1	65.66		29.19	K	74.43	
62.88	M_1	65.69		67.22	L_2	74.24	
65.18	N_1	65.77		74.04	N_2	74.30	74.3
	average	65.70	65.71±0.01				
				51.72	K	96.92	
55.65	L_1	67.74		89.61	L_1	97.04	97.0
57.55	L_3	67.75					
	average	67.75	67.74±0.01	69.05	K	114.25	
				106.76	L_1	114.19	
30.60	K	100.11		107.77	L_3	114.23	
88.49	L_2	100.03		112.60	M_1	114.25	
89.82	L_3	100.02		113.97	N_1	114.31	114.25
97.73	M_3	100.00					
99.67	N_3	100.09		96.96	K	139.16	139.2
	average	100.05	100.09±0.02				
				110.68	K	155.88	155.9
44.11	K	113.62	113.66±0.02				
				143.45	K	188.65	188.7
				146.85	K	192.05	192.1
				153.71	K	198.91	198.9
				162.82	K	208.02	
				200.53	L_1	207.96	208.0
				165.96	K	211.16	
				203.85	L_1	211.28	
	Ta^{183}			209.61	M_1	211.26	211.23
34.36	L_1	46.45	46.48±0.01				
45.88	N_1	46.47		194.89	K	240.09	
				232.71	L_1	240.14	
40.46	L_1	52.55	52.59±0.01	238.61	M_1	240.26	240.15
38.38	K	107.89	107.93±0.02	222.43	K	267.63	
				260.16	L_1	267.59	267.6
				224.90	K	270.10	270.1

TABLE III. Energies (in keV) of internal-conversion lines observed on Nd^{149} plates.

Electron energy	Assignment	Transition energy	Average	Comments
23.07	L_2	30.09		
23.59	L_3	30.05		
28.69	M_3	30.04	30.05	
29.25	K	74.36		
67.26	L_2	74.28		
67.80	L_3	74.26		
72.89	M_2	74.35		
74.24	N_2	74.50	74.30	
31.62	K	76.82	76.8	
51.78	K	96.98		
89.66	L_1	97.09		
95.38	M_1	97.03		
97.01	N_1	97.35	97.03	
69.12	K	114.32		
106.91	L_1	114.34		
107.87	L_3	114.33		
112.68	M_1	114.33		
114.14	N_1	114.48	114.33	
77.34	K	122.54	122.5	
94.06	K	139.26		
131.82	L_1	139.25	139.3	Could also be K for 177.0-keV transition.
110.71	K	155.91		
148.49	L_1	155.92	155.91	
143.59	K	188.79		
181.63	L_1	189.06		Also K for transition of 226.8 keV.
187.19	M_1	188.84	188.8	
146.91	K	192.11	192.1	
153.77	K	198.97		
191.78	L_1	199.21		
197.00	M_1	198.65	198.9	
163.03	K	208.23	208.2	
166.11	K	211.31		
204.03	L_1	211.46		
209.76	M_1	211.41		
210.95	N_1	211.29	211.38	
168.84	K	214.0	214.0	
181.63	K	226.83	226.8	Also L_1 for 188.8 keV.
184.86	K	230.06	230.1	Could also be L_1 for 192.3.
195.07	K	240.27		
232.94	L_1	240.37		
238.73	M_1	240.38	240.33	
200.70	K	245.90	245.9	Could also be L_1 for 208.1.
222.50	K	267.70		
260.41	L_1	267.84		
266.02	M_1	267.67	267.7	
225.08	K	270.28	270.3	
230.36	K	275.56	275.6	
243.05	K	288.25	288.2	
281.46	K	326.66	326.7	
378.74	K	423.94	423.9	Better energy from Ge data.
496.36	K	541.56	541.6	Better energy from Ge data.
239.15	K from Pm^{149}	286.00	286.0	

where two uniquely interpreted conversion lines are observed for one transition, these Nd^{149} transition energies are accurate to about 1 part in 2000 above 100 keV and to 0.05 keV below 100 keV. For the other transitions the uncertainties are assumed to be about twice as large.

A list of the conversion lines observed with sources of Nd^{149} is given in Table III along with the interpretations. These Nd^{149} energies should be reduced by 1 part in 3000, so that the transitions in common have the same average energy as those in Tables I and II. (This correction is of the same magnitude as that for the tantalum plates.) The average transition energies from these two sets of data are included in a later tabulation of transition energies and intensities (Table VI). Several other lines were observed on two or three plates but have not been interpreted unambiguously. These lines are at 34.7, 46.0, 58.1, 71.7, 84.1, 88.7, 92.1, and 228.1 keV.

TABLE IV. Relative internal-conversion-electron intensities.

Transition energy (keV)	Line	Intensity: Spectrograph plates	Intensity: Solid-state detector
97.0	K	1.5 ±0.8	~1
114.3	K	16.5 ±2.5	≡16.5
	L	2.3 ±0.4	
	M	0.55±0.1	
	N	0.2 ±0.1	3.4 ±0.6
155.9	K	0.35±0.15	
188.8	K	0.30±0.10	≤0.35
198.9	K	0.20±0.07	...
211.4	K	4.4 ±0.8	4.1 ±0.3
	L	0.65±0.15	
	M	0.15±0.08	3.4 ±0.4
240.3	K	≡2.4	
	L	0.41±0.08	1.14±0.4
267.6	K	0.58±0.1	
	L	0.11±0.05	...
270.2	K	0.18±0.06	
326.6	K	0.12±0.06	...
423.5	K	0.08±0.08	...

TABLE V. Gamma-ray energies between 300 and 700 keV. Spectrum of Nd^{149}, Au^{198}, Na^{22}, Cs^{137}.

Photopeak position (channels)	Correction to channel	Energy (keV)	
298.69±0.02	−1.65	≡211.32	
339.86±0.03	−1.70	240.26 ±0.2	
379.06±0.09	−1.72	267.84 ±0.2	
382.52±0.05	−1.72	270.27 ±0.2	
462.48±0.02	−1.65	326.59 ±0.2	
494.48±0.07	−1.60	349.15 ±0.2	
583.35±0.01	−1.38	411.84 ±0.15	(Au^{198})
600.08±0.02	−1.32	423.66 ±0.2	
628.29±0.04	−1.22	443.58 ±0.2	
723.63±0.03	−0.76	≡511.005	(Na^{22})
765.38±0.03	−0.49	540.57 ±0.2	
787.74±0.08	−0.34	556.42 ±0.2	
926.40±0.20	+0.77	654.81 ±0.4	
936.12±0.02	+0.87	661.72 ±0.2	(Cs^{137})

Conversion-Electron Intensities

Three sets of spectrographic plates were used to determine the relative electron-line intensities. These sets of plates were obtained with sources whose thick-

TABLE VI. Gamma-ray transition energies and intensities.

Transition energy (keV)	Photon	Conversion electron	Transition	Transition energy (keV)	Transition intensity
30.00±0.05				540.5±0.2	6.5 ±0.6
59.0 ±0.3	~0.8			556.4±0.2	1.1 ±0.2
74.4 ±0.2	2.1 ±0.4			581 ±1	0.15 ±0.05
76.8 ±0.2	1.4 ±0.2			~600	<0.1
97.02±0.1		2	~3	631 ±1	0.2 ±0.1
114.30±0.05	19 ±2	19	38	654.7±0.4	≡8.4
122.5 ±0.2	~0.15			686 ±2	0.05 ±0.02
126.5 ±1	~0.05			696 ±2	0.09 ±0.03
139.2 ±0.1	0.5 ±0.1			712 ±2	0.07 ±0.02
155.9 ±0.1	5.8 ±0.6	0.4	6.2	~755	<0.2
177.8 ±1	~0.2			~770	
188.8 ±0.1	1.7 ±0.3	0.3	2.0	810 ±1	0.22 ±0.05
192.1 ±0.2	0.4 ±0.2			~830	
198.9 ±0.2	1.2 ±0.3	0.2	1.4	~840	<0.2
208.2 ±0.2	2,6 ±0.5			~860	
211.32±0.1	24 ±2	5.0	29	925 ±2	0.09 ±0.03
214.0 ±0.3	0.2 ±0.15			980 ±2	0.08 ±0.02
226.8 ±0.5	0.1 ±0.05			1026 ±2	0.11 ±0.03
230.1 ±0.5	0.5 ±0.2			1043 ±5	0.006±0.004
240.25±0.15	3.8 ±0.4	2.7	6.5	1080 ±2	0.06 ±0.02
245.9 ±0.3	0.8 ±0.2			1103 ±2	0.04 ±0.02
258 ±1	0.4 ±0.1			1128 ±3	0.04 ±0.02
267.7 ±0.2	6 ±1	0.7	7	1176 ±3	0.014±0.006
270.3 ±0.2	10 ±1	0.2	10	1201 ±3	0.015±0.005
275.6 ±0.4	0.5 ±0.2			1237 ±2	0.04 ±0.02
282.6 ±0.5	0.4 ±0.2			1266 ±3	0.010±0.005
288.2 ±0.3	0.4 ±0.2			1291 ±3	0.004±0.002
294.9 ±0.5	0.6 ±0.1			1314 ±2	0.006±0.003
301.2 ±0.5	0.4 ±0.1			~1336	~0.001
311.0 ±0.5	0.4 ±0.1			1359 ±3	0.003±0.001
326.6 ±0.2	4.4 ±0.4	0.1	4.5	1384 ±3	0.002±0.001
349.1 ±0.2	1.5 ±0.2			1456 ±3	0.002±0.001
366.5 ±1.5	0.5 ±0.15				
385 ±2	0.3 ±0.1				
423.6 ±0.2	7.0 ±0.7				
443.5 ±0.2	1.1 ±0.2				
~480	<0.3				
~490					

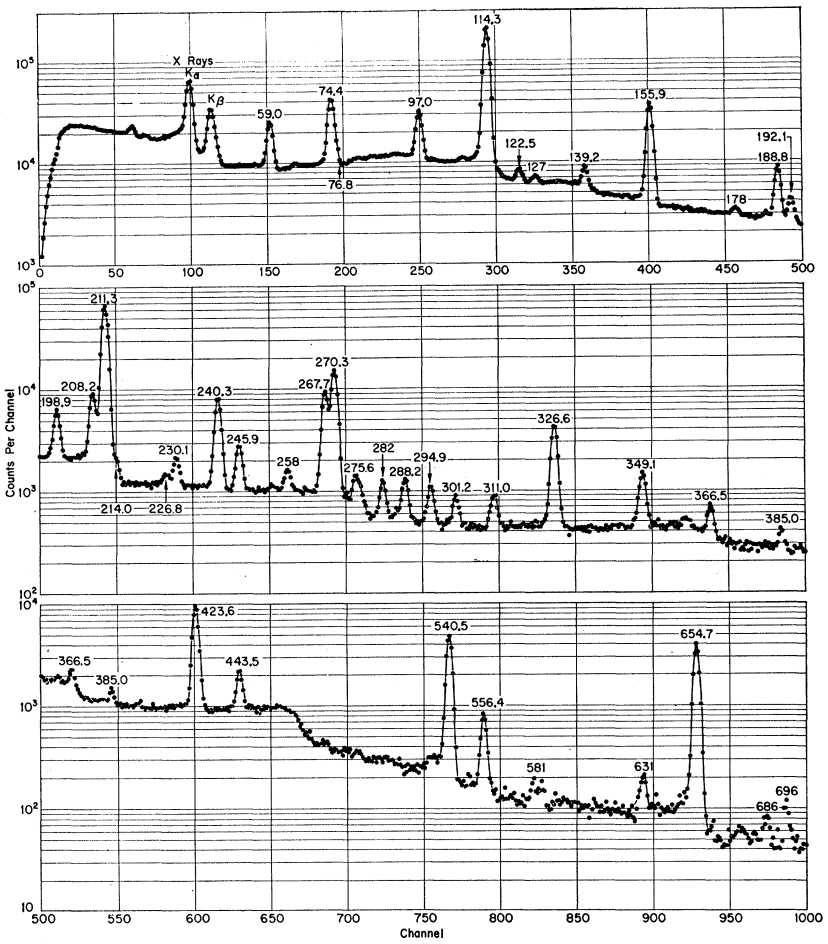

FIG. 2. Low-energy portion of gamma-ray spectrum of Nd^{149} measured with germanium detector. The germanium detector was 4 mm thick. For the two upper sections, it had a resolution of about 1.8 keV and 2.8 keV for the bottom section.

nesses were estimated by activation methods to be 0.01, 0.3, and 1 mg/cm². Only the most intense lines (K-114, L-114, K-211, and K-240) could be observed with the thinnest source. The line shapes were all the same and were fairly symmetric for this source. For the thicker sources large low-energy tails were observed and the low-energy lines were wider than the others. The results of these measurements are given in Table IV. The errors quoted are subjective estimates of the quality of the data and the uncertainties in the corrections.

Although the poorer resolution of the electron spectrum taken with a silicon surface-barrier detector (see, for example, Fig. 6) does not allow one to see the individual lines, the results do provide a check on the over-all intensities from the plates. These values are included in Table IV. The associated errors include only the estimated uncertainty in determining the areas of the observed peaks.

Gamma-Ray Energies

The energies of most of the transitions below 300 keV can best be determined from the conversion-electron measurements. Between 300 and 670 keV, the energies were obtained from spectra, such as that shown in Fig. 1, from lithium-drifted germanium detectors. The peak positions, corrections for analyzer nonlinearity, and resulting energies for one such spectrum are given in Table V. The peaks at 211.32 (Nd^{149}) and 511.01 keV (Na^{22}) were used as energy calibration points. Since the energies of the peaks at 411.79 (Au^{198}) and 661.6 (Cs^{137}) keV agree with reported values to 0.05 and 0.1 keV, it is assumed the calibration is accurate to 0.15 keV. This value plus twice the computed uncertainty in the peak position is taken as the error in the transition energy.

Above 670 keV the transition energies were taken from a gamma-ray spectrum of Nd^{149} from a germanium detector (Fig. 3). The long counting time required precluded an internal calibration, but calibration spectra were taken before and after the Nd^{149} run. These energies are given in Table VI.

Gamma-Ray Intensities

The gamma-ray spectra of Nd^{149} samples as measured with lithium-drifted germanium detectors are shown

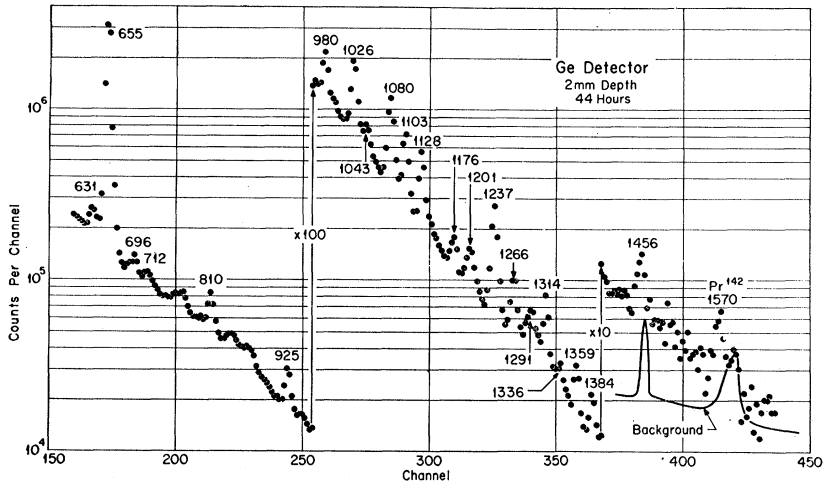

FIG. 3. High-energy portion of Nd^{149} gamma-ray spectrum obtained with a germanium detector 2 mm thick with 5-keV resolution.

in Figs. 2 and 3, and the spectrum from a NaI(Tl) detector is shown in Fig. 4. The spectra from the germanium detector were taken with sources that had been purified by ion-exchange column separations, so that only Nd^{149} (1.7 h), Pm^{149} (53 h), and Nd^{147} (11 day) were present. It was shown that there is no observable contribution from Nd^{147} or Pm^{149}. For the count rates and geometry used, the random and coincidence summing should both be negligible.

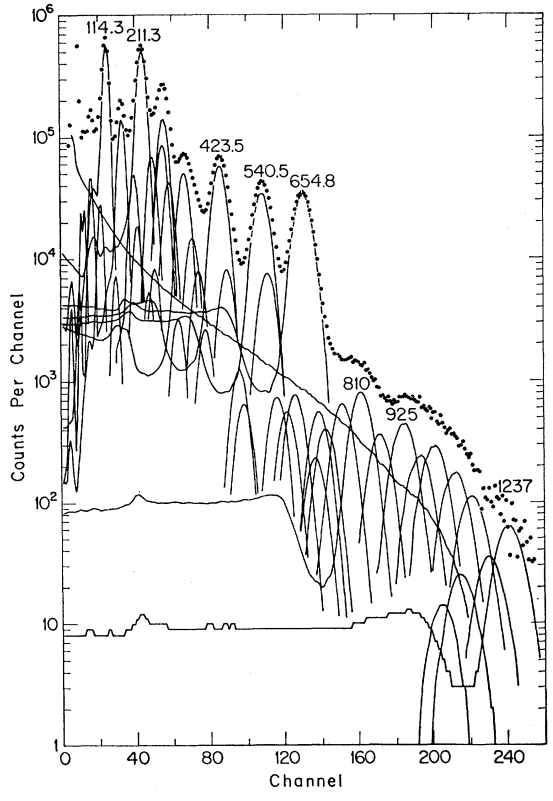

FIG. 4. Analysis of Nd^{149} gamma-ray spectrum from a 3-in. ×3-in. NaI(Tl) detector. See text and Appendix for discussion of analysis.

The relative gamma-ray intensities were determined by means of the spectra from both detectors. The analysis is described in the Appendix. The results are listed in Table VI and are shown in Fig. 4. The relative gamma-ray intensities were converted to absolute intensities with the aid of a 4π β-γ coincidence measurement. From these data the intensity of the 655-keV gamma ray was found to be 8.4 ± 0.5 percent of decays. This value includes a correction for the fact that the 240-keV transition has a 41 μsec half-life. The simple 4π β-γ coincidence result was increased by 7% to account for the presence of conversion electrons and gamma rays that are not in coincidence with the beta rays.

Half-Life of 240-keV Transition

Several experiments indicated that the 240-keV transition might have a lifetime greater than $\frac{1}{2}$ μsec. The 4π β-γ coincidence system was used to investigate this possibility. This system has a normal resolving time of $2\tau=4$ μsec. Each pulse from the 4π β counter was used as a gating signal and the output of the NaI detector was fed to a multichannel analyzer. In the first experiment, the beta pulse was used to turn the analyzer off (i.e., in anticoincidence mode). A typical anticoincidence spectrum is shown in Fig. 5 along with a singles spectrum. The enhancement of the 240-keV transition indicates that its lifetime, or that of some previous transition, is greater than 1 μsec. The half-life of this transition was then determined by a series of β-γ coincidence measurements in which the beta pulse was delayed by various amounts. The results for the intensity of the 240-keV transition are shown in Fig. 5. This half-life of (41 ± 10) μsec implies an $M2$ transition which is slower than the single-particle lifetime

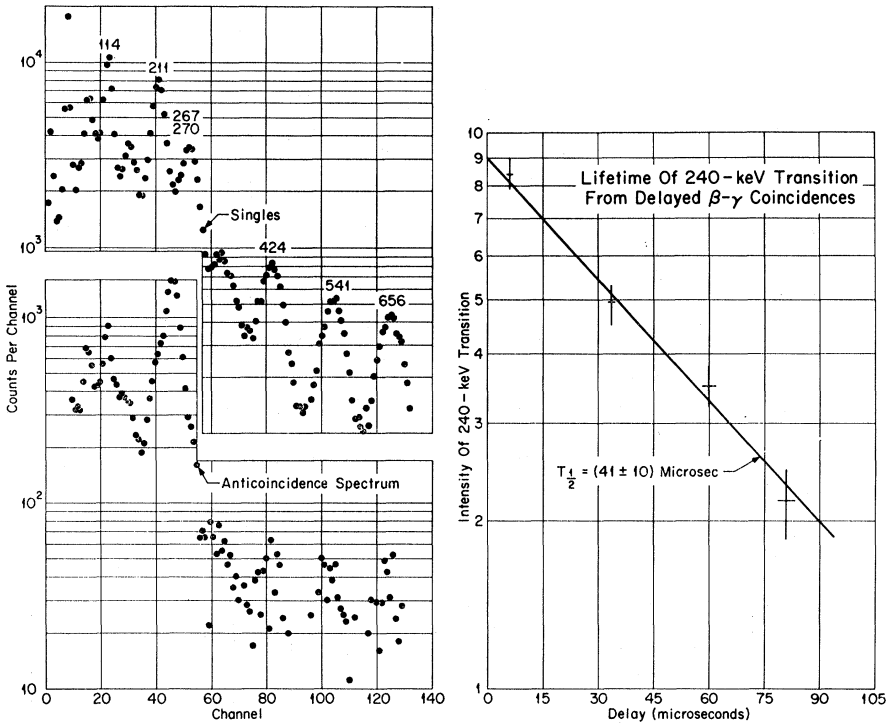

FIG. 5. Left portion shows gamma-ray spectrum in anticoincidence with beta rays. The half-life of the 240-keV transition is shown on the right.

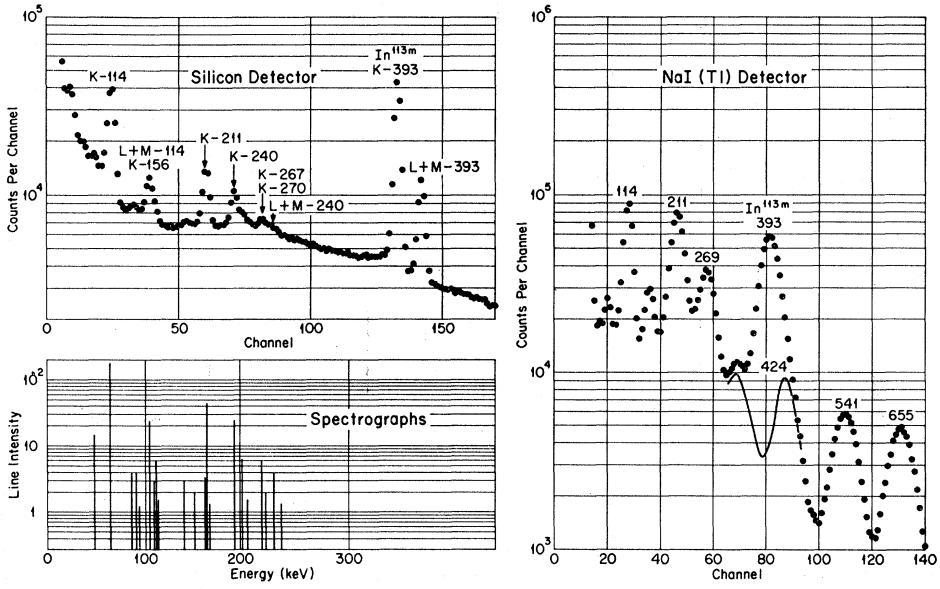

FIG. 6. Electron spectrum of Nd^{149} and In^{113m} as measured with a silicon detector.

estimate of Moszkowski[15] by a factor of about 80. This hindrance factor is consistent with that of other observed $M2$ transitions. For example, most of the hindrance factors shown by Goldhaber and Sunyar[16] range from 10 to 300 with median near 100.

[15] S. A. Moszkowski, in *Alpha-, Beta-, and Gamma-Ray Spectroscopy*, edited by Kai Siegbahn (North-Holland Publishing Company, Amsterdam, 1965), Vol. 2, Chap. XV.

[16] M. Goldhaber and A. W. Sunyar, in *Alpha-, Beta-, and Gamma-Ray Spectroscopy*, edited by Kai Siegbahn (North-Holland Publishing Company, Amsterdam, 1965), Vol. 2, Chap. XVIII, Fig. 9, p. 945.

TABLE VII. Internal-conversion coefficients.

Transition (keV)	Coefficient	Experimental value	Theoretical values $M1$	$E2$	$E1$	$M2$	Multipolarity
30.0	L_1/L_2	<1	11	0.004	1.7	13	$E2$ (<2% $M1$ mixture)
	L_2/L_3	≥0.5 and ≤2	5	0.7	0.65	0.15	
97.0	α_K	1.1 ±0.4	1.5	1.3	0.27	15	$M1$ (or $E1+M2$ mixture)
	L_1/L_3	>3	60	0.25	4.1	5.4	
114.3	α_K	0.9 ±0.2	0.94	0.79	0.17	8.0	$M1$ (≤2% $E2$ mixture)
	K/L	7 ±1	7.4	1.65	7.0	4.3	
	L_1/L_3	>20	66	0.37	5	6	
155.9	α_K	0.05±0.03	0.40	0.34	0.075	2.6	$E1$
211.3	α_K	0.18±0.03	0.165	0.13	0.031	0.86	$M1$ (with ≤20% $E2$ mixture or $E1+M2$)
	K/L	7 ±1	6.9	3.7	7.2	5.5	
	L_1/L_3	>5	50	1.3	7.7	11	
267.7	α_K	0.09±0.03	0.085	0.063	0.016	0.39	$M1$ or $E2$ (or $E1+M2$)
	K/L	5.5 ±2	6.9	4.4	7.2	6.0	
270.0	α_K	0.02±0.01	0.085	0.063	0.016	0.39	$E1$
326.6	α_K	0.03±0.02	0.052	0.032	0.010	0.20	
423.5	α_K	0.01±0.01	0.025	0.015	0.005	0.085	

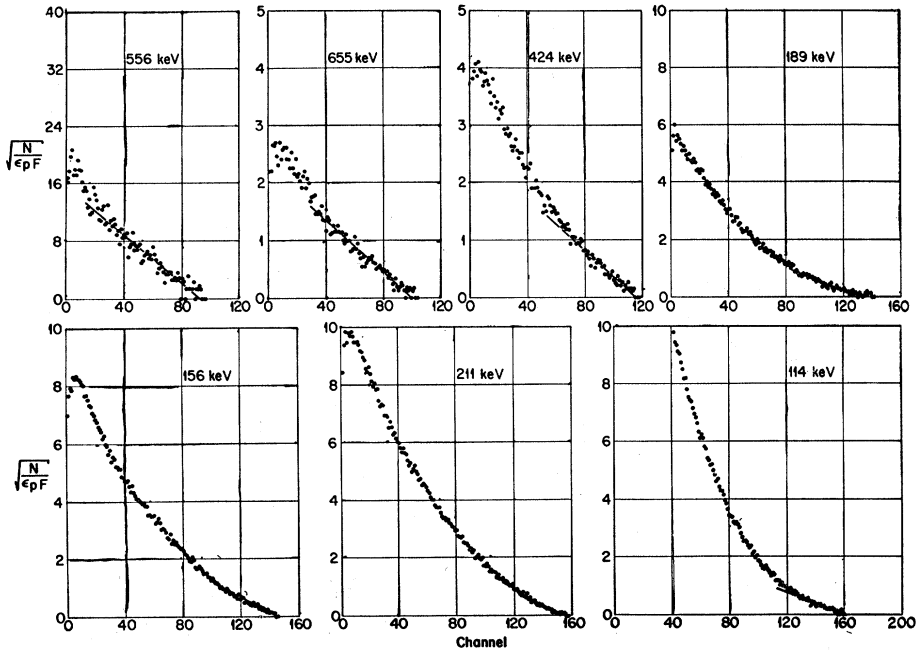

FIG. 7. Fermi plots of beta-ray spectra in coincidence with the gamma-ray peaks noted.

Internal-Conversion Coefficients

By proper normalization of the relative intensities in Tables IV and VI, the internal-conversion coefficients of several transitions can be determined. A preliminary normalization was carried out by means of a mixed source of Nd^{149} and In^{113m}. Gamma-ray and electron spectra from one such source are shown in Fig. 6. For the In^{113m} transition, a value of $\alpha_K=0.44$ from Ref. 17 was used. From this value and the relative intensities, $\alpha_K=0.65\pm0.3$ was obtained for the 240-keV transition. This result together with the values of $K/L\geqslant5$ and $L_1/L_3\gtrsim3$ (visual estimate) imply that this transition has $M2$ character. This conclusion is in agreement with the half-life determined for this transition.

The relative gamma-ray and conversion-electron intensities were then normalized by means of the theoretical conversion coefficient[18] for this $M2$ transition, $\alpha_K=0.58$. The resulting conversion coefficients and K/L ratios are shown in Table VII along with the theoretical coefficients.[18]

[17] S. C. Misra, J. S. Merritt, and J. G. V. Taylor, Atomic Energy of Canada, Limited, Report AECL-2256, 1965, p. 23 (unpublished).

[18] L. A. Sliv and I. M. Band, Part I, K shell, AEC-tr-2888, 1956, and Part II, L shell, NP-tr-217, 1958 (unpublished).

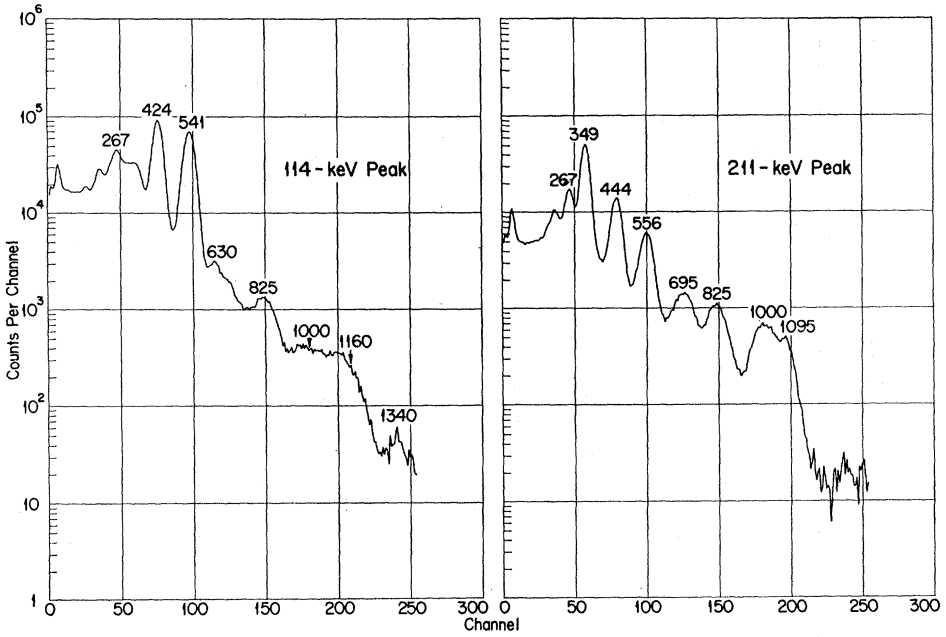

FIG. 8. Gamma-ray spectra in coincidence with peaks at 114 and 211 keV. A lead absorber has attenuated low-energy portion of spectrum. The energies shown are those of the peaks and not those of coincident gamma rays. These are plots of the actual data points with a straight line between the points.

One of the more sensitive indications of a gamma-ray multipolarity is the relative intensity of the three L subshell conversion lines. For several transitions, these ratios were estimated from visual examination of the spectrograph plates and from analysis of the microphotometer traces. These results are included in Table VII. The multipolarities deduced are shown in the last column of the table.[18a]

Nd^{149} Half-Life

The half-life of Nd^{149} was measured by use of the integral, gamma-ray count from a NaI(Tl) detector. The sample was purified and then counted for more than ten half-lives. The data were analyzed on the assumption of the presence of three components Nd^{149} ($T_{1/2}$ and intensity calculated), Pm^{149} (intensity calculated and $T_{1/2}$ given), and the background (intensity and $T_{1/2}$ given). The resulting value of $T_{1/2}=(1.73\pm0.01)$ h agrees with the value of (1.72 ± 0.01) h reported by Rider *et al.*[5]

COINCIDENCE EXPERIMENTS

Beta-Gamma Measurements

A portion of the results of a β-γ coincidence experiment are shown in Fig. 7. The original data have been reduced to Fermi plots, but no corrections have been made for the detector resolution or backscattering of electrons out of the detector. These spectra indicate the presence of seven different beta-ray branches. The end-point energies were determined by comparison with those from the decay of Eu^{154}. In all cases comparison of these spectra with those in coincidence with the underlying Compton distribution, indicated that the latter did not interfere with the endpoint measurement. The results are given in Table VIII. A comparison of the beta-ray singles spectrum with that in coincidence with the 114-keV transition indicates that any ground-state beta-ray branch is weak.

Gamma-Gamma Measurements

The γ-γ coincidence data result from three experiments. In two of these, two NaI(Tl) detectors were used and the data were stored in a 256×256 channel array. In the first experiment both analyzers spanned the region below 800 keV. The crystals were mounted

TABLE VIII. Beta-ray branches observed in beta-gamma coincidence runs.

Gating gamma ray (keV)	Beta endpoint energy (MeV)	Energy expected from decay scheme (MeV)
556	0.92	0.90
655	1.00	1.01
541	1.02	
424	1.13	1.13
326	1.12	
349	1.10	
188	1.30	1.28
270	1.36	1.40
156	1.40	
211	1.47	1.45
114	1.56	1.55

[18a] *Note added in proof.* Recently Bäcklin *et al.* [A. Bäcklin, H. Solhed, and M. C. Joshi (private communication)] have reported the following multipolarities 74($E2$+$M1$), 81($E1$), 97($M1$), 114($M1$), 155($E1$), 188($E2$), 198($M1$), 208($M1$,$E2$), 211($M1$+$E2$), 240($M2$), 267($M1$), 270($E1$), 326($E1$,$E2$), 423($E1$,$E2$), 541 keV ($M1$,$E2$).

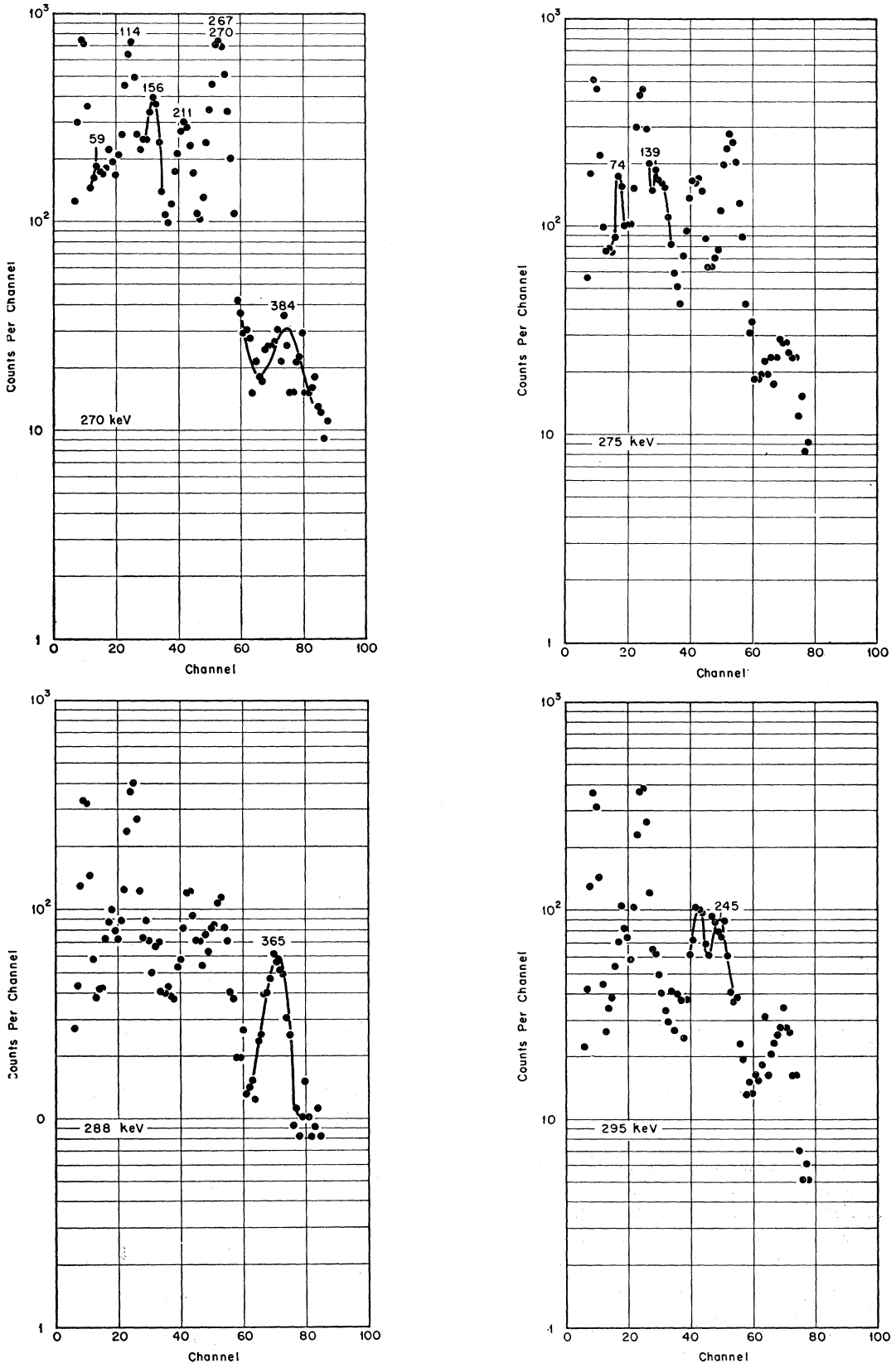

FIG. 9. Gamma-ray spectra in coincidence with various energy ranges around 280 keV. The gating pulses are from a germanium detector. Only the transitions in coincidence with the gamma ray in the gating windows are labeled. The first gate includes both the 267- and 270-keV transitions.

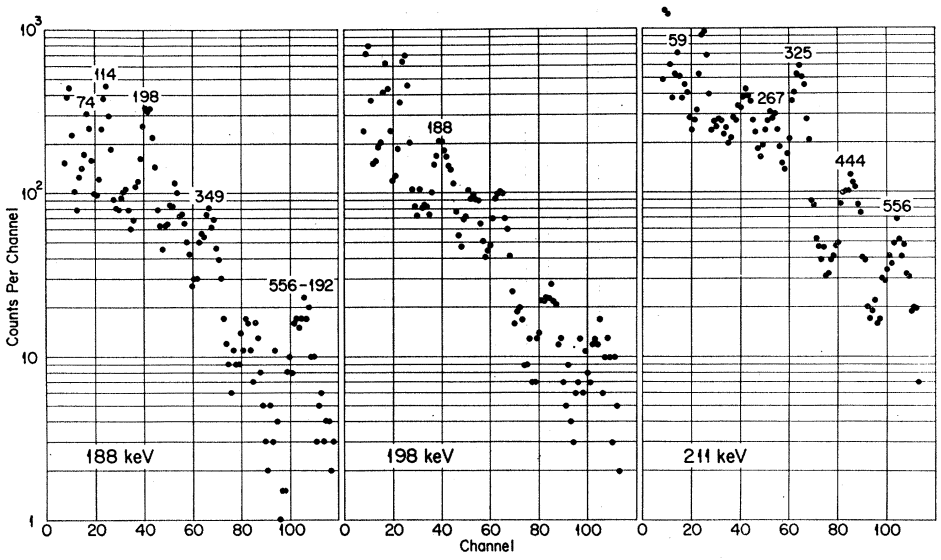

FIG. 10. Gamma-ray spectra in coincidence with the pulses in the 200-keV region. The gating pulses are from a germanium detector.

TABLE IX. Gamma-gamma coincidence results. An X represents an observed coincidence relationship and an O one which is not observed. A blank indicates a lack of definitive information.

E_γ (keV) \ E_γ (keV)	59	74 76	97	114	139	156	189 192	198	211 208 214	246 255	268 270	288	295 301	326	349	365	385	424	444	480	540	556	581
74, 76		X																					
97	X																						
114	X	X	X																				
156				X																			
198		X				O	X																
211, 208, 214	X						X		X														
268, 270	X			X		X			X	O	X												
275		X			X																		
295, 301										X													
326	O		X	X		O			X	O	O	O											
349		X		X			X				O	O		O									
366				O							O	X		O	O								
385											X												
424	O			X		O	O	O	O	O	O	O		O	O	O	O						
444				O				O	X	O	O	O		O	O	O	O	O					
480									X											X			
541	O		O	X		O	O	O	O	O	O	O		O	O	O	O	O	O				
556				O			X	O	X	O	O	O		O	O	O	O	O	O		O		
581																					X		
631																				X			
655	O		O	O		O	O	O	O	O	O	O		O	O	O	O	O	O		O	O	X
686, 696									X		X			X	X			X				X	
810									X		O		X	O				X			O		
850							X	X			X												

with their axes at an angle of 90°. A lead shield, covered with tantalum and cadmium, was placed between the detectors to prevent crystal-to-crystal scattering. In the second experiment, the analyzers spanned the regions up to 1000 and 1400 keV. The crystals were oriented at 180°, but one had a 2-g/cm² lead absorber to prevent intercrystal scattering. Typical spectra from the second of these two experiments are shown in Fig. 8. The third experiment consisted of a series of measurements in which one of the detectors was replaced by a lithium-drifted germanium detector. In this case, the spectra were stored in the 4096-channel memory. Samples of the resulting spectra are shown in Figs. 9 and 10.

The coincidence relationships deduced from these experiments are summarized in Table IX. The results for the 810-keV transition cannot be explained simply. They imply either the main portion of the decay scheme

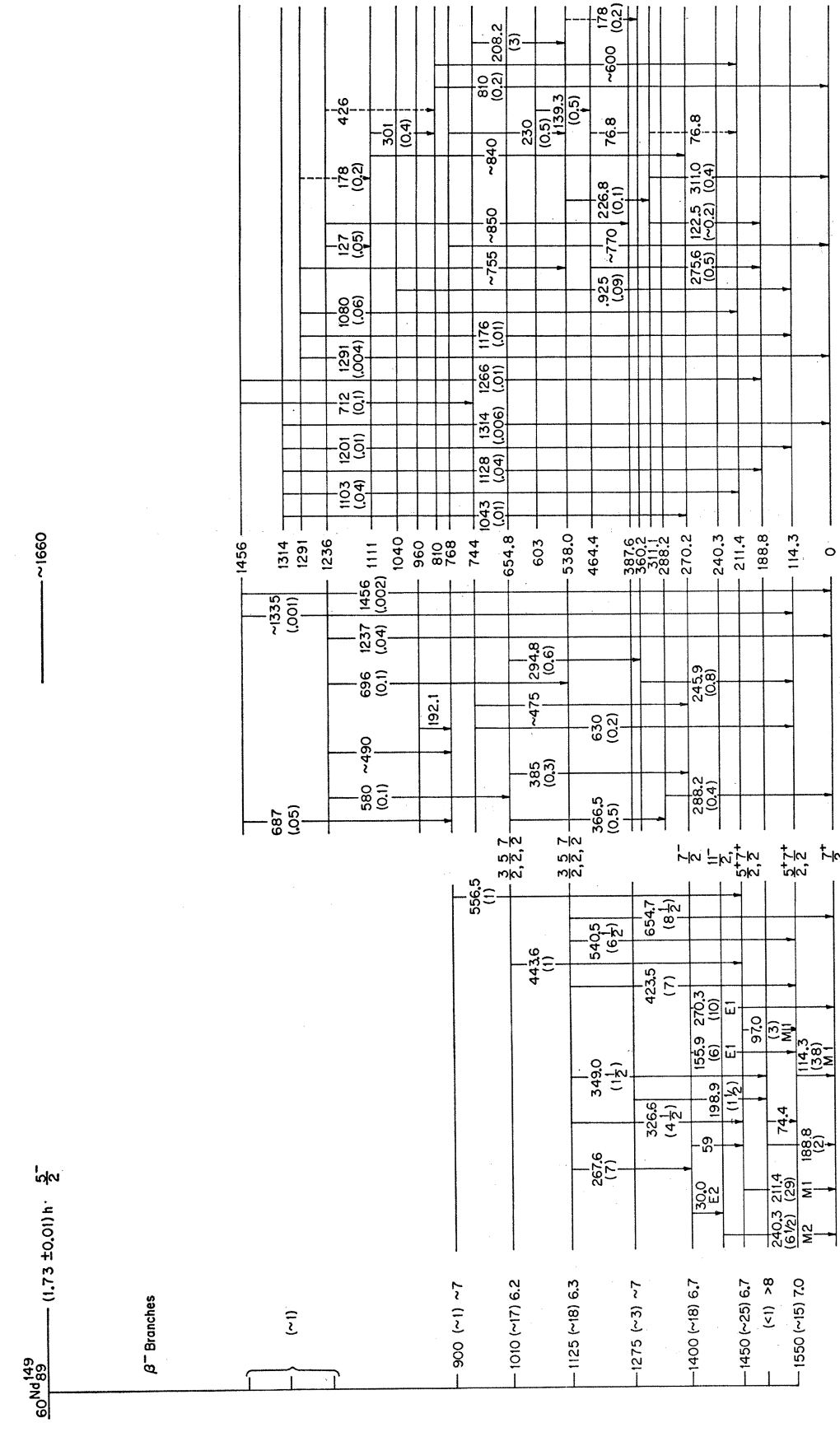

FIG. 11. Proposed decay scheme. The energies are in keV and the intensities in percent of decays are in parentheses. The beta-ray branches are shown at the left. Their intensities are deduced from the gamma-ray intensities. The ground-state spins have been measured. For the other levels a set of possible spins is shown (see text). The dashed transitions represent two placements for the same gamma ray.

TABLE XI. Hindrance and enhancement of several gamma-ray transitions.

Initial level (keV)	Level lifetime[a] (sec)	Transition (keV)	Branching %	Total conversion coeff.	Experimental photon lifetime (sec)	Multipolarity	Single-particle lifetime	Hindrance≡ (experimental lifetime)/(single-particle lifetime)
114	3×10^{-9}	114	100	1.3	7×10^{-9}	$M1$	1.6×10^{-11}	400
270	3×10^{-9}	270	40	0.02	7×10^{-9}	$E1$	1.2×10^{-14}	6×10^{5}
		156	24	0.06	12×10^{-9}	$E1$	6.4×10^{-14}	2×10^{5}
		59	8[b]	~1.2	53×10^{-9}	$E1$[b]	1.2×10^{-12}	0.5×10^{5}
		30	28[b]	400	4×10^{-6}	$E2$	4.8×10^{-4}	1/80

[a] Values are from Ref. 6.
[b] Assumed values.

(Fig. 11) is incorrect, or that there is a second transition of about 425 keV. The latter alternative is preferred, and is shown in the right section of the scheme. The resolution on the coincident radiations, above 1 MeV (Fig. 8) is not sufficient to determine explicit relationships. However, these spectra do indicate the energy ranges of the transitions in coincidence with the strong, low-energy gamma rays.

Some coincidence relationships are illustrated by the results discussed in the Appendix (Fig. 13).

DISCUSSION

Decay Scheme

The proposed decay scheme is given in Fig. 11. The left-hand portion of the scheme is considered to be well established by this study. All coincidences are unambiguously observed, except those involving the 30-keV transition. The center section is believed to be correct. The coincidences implied by this portion are observed. However, in some cases the experiments do not uniquely establish the order and position of a cascade. The right-hand portion of the scheme is put together primarily from energy considerations and is tentative. As shown in Table IX a few of the implied coincidences are observed. Since the coincidence relationships involving most of the transitions above 1 MeV are not uniquely determined, they are shown in this section. However, the good agreement of the sums of the energies of the cascades from the 1314-keV level is good evidence for the existence of this state and for most of the cascades from it.

The beta-ray intensities are computed from the gamma-ray transition intensities and the decay scheme. The total intensity of the transitions feeding the ground state is, as shown, about 95%. This is consistent with the beta-gamma coincidence measurements which indicate that the beta branch to the ground state is weak. The logft values of 6-7 for the observed beta-ray transitions (see Table VIII) imply that these transitions all have nonunique first-forbidden or hindered allowed character.

The agreement in energy between some of the cascade and crossover combinations is shown in Table X. Only those transitions whose energies were obtained from the magnetic spectrographs or the germanium detector are included in the table.

The 240-keV level is of special interest. No coincidences are observed with the 240-keV gamma ray. This is taken to mean that this transition goes to the ground state or to some low-energy level. From the energy sum, it is assumed that the 30- and 240-keV transitions are in cascade from the 270-keV level. Since the 240-keV transition has a half-life of 41 μsec and

TABLE X. Sum–crossover comparisons.

Gamma-ray energies with errors of 1 keV or more are included in the lower section.

Gamma No. 1 (keV)	Gamma No. 2 (keV)	Crossover (keV)	Sum–crossover difference (keV)
97.02	114.30	211.32	0.00
114.30	74.4	188.8	0.1
114.30	155.9	270.3	0.1
30.00	240.25		0.0
76.8	198.9	275.6	0.1
114.30	423.6	537.9[a]	0.0
188.8	349.1		0.0
211.32	326.6		0.0
267.7	270.3		0.1
114.30	540.5	654.7	0.1
211.32	443.5		0.1
288.2	366.5		0.0
155.9	267.7	423.6	0.0
97.0	326.6		0.0
97.0	443.6	540.5	0.1
288.2	366.5	654.7	0.0
270.3	384		~0.5
654.7	581	1237	1
537.9[b]	696		3
211.32	1026		0
211.32	1080	1291	0
114.30	1176		1
270.3	1043	1314	1
211.32	1103		0
188.8	1128		3
114.30	1201		1
211.3+556.4	686	1456	2
114.3+631	712		1

[a] Average value of sums.
[b] Level energy.

that of the 270-keV level is 3 nsec,[6,7] the 30-keV transition must depopulate the 270-keV state. The long lifetime of the 240-keV state prevented the observation of the beta-ray transition feeding, directly or indirectly, the 240-keV level. Also, the low energy of the electrons from the 30-keV transition prevented the measurement of their intensity by the techniques available. On the basis of the spin arguments of the next section, it is assumed that there is no beta-ray branch to the 240-keV level and that the 30-keV transition has an intensity of about 6.5%.

The level shown at 288 keV could also be placed at 366.5 keV. Then the transitions of 925, 127, and 178 keV could be placed between this level and those at 1291, 240.3, and 188.8 keV, respectively. There is no coincidence information on any of these three transitions.

From the lifetime measurements in Ref. 6 and the multipolarities and relative intensities determined here, several gamma-ray lifetimes can be estimated. These are given in Table XI. Although the results indicate large hindrances for the $E1$ transitions, these values are within the range previously observed. Of particular interest is the 30-keV transition which appears to be an $E2$ with an enhancement of about 80. If there is a beta-ray branch to the 240-keV state this enhancement will be less, but the transition will still be significantly enhanced.

The gamma-ray coincidence experiments indicate strong 75-75- and 198-75-keV coincidences. These are interpreted as resulting from the 76.8-198.9-74.4 cascade. Other authors[3,6] have proposed an 81-keV transition between the 270- and 188-keV levels. No conversion lines were observed for such a transition. This transition would also imply coincidences between the 267- and 188-keV transitions. These were not observed. The reported[1,2,6] transition of about 112 keV was also not observed.

Spins and Parities

The spin of the ground state of $_{60}Nd_{89}^{149}$ has been measured[19] to be $\frac{5}{2}$. Since in the shell model,[20] the seven neutrons after the closed shell at 82 should be in the $f_{7/2}$ level, one would expect a $\frac{7}{2}^-$ state. Thus, it seems more likely that the Nd^{149} nucleus is deformed.[21] In this case, for a deformation of $\delta\approx 0.04$, the $\Omega=\frac{5}{2}$ Nilsson level from the splitting of the $f_{7/2}$ state is available. Therefore, it is presumed that Nd^{149} has a small deformation with a positive value of δ and negative parity.

The ground-state spin of $_{61}Pm_{88}^{149}$ has been measured[22] to be $\frac{7}{2}$. The shell model indicates the presence of the $d_{5/2}$ and $g_{7/2}$ states after the closed shell at 50 protons. The measured spins[23] for ground states of $_{57}La^{139}$ and $_{61}Pm^{147}$ are $\frac{7}{2}$, while those for $_{59}Pr^{141}$, $_{61}Pm^{151}$, and $_{63}Eu^{151}$ are $\frac{5}{2}$. In most of these nuclei, the transitions between the first excited states and the ground states are $M1$ which are usually retarded. The hindrance would be explained by the $\Delta l=2$ of the $d_{5/2}\leftrightarrow g_{7/2}$ transition. Similarly, in Pm^{149} the 114-keV transition is hindered by a factor of $\sim$400. The ground-state spin can also be explained simply for a nucleus with a small deformation. The level ordering[21] has the $\Omega=\frac{7}{2}$ level from the $g_{7/2}$ state available for $\delta\approx 0.05$. Therefore, it is concluded that in Pm^{149} the 61st proton is either in a $g_{7/2}$ level or in an $\Omega=\frac{7}{2}$ Nilsson level. In either case the parity is positive.

From the $M2$ character of the 240-keV transition, there are two possible spins, $11/2^-$ and $\frac{3}{2}^-$, for this level. The former spin would imply a unique, second-forbidden beta transition to this level, while the $\frac{3}{2}^-$ assignment would imply an allowed beta transition. For the allowed transition one would expect a logft of <6.7 or a beta intensity of $>20\%$ of the decays. The intensity of the 240-keV transition is about 7% of the decays. Thus if the spin and parity are $\frac{3}{2}^-$, the beta decay must be strongly hindered. Therefore, chosing the more likely case it is presumed that the 240-keV level has spin and parity $11/2^-$.

The general lack of transitions from or to the 240-keV level suggests that, if the $11/2^-$ assignment is correct, the other states have spins of $\frac{7}{2}$ or less. The $E2$ assignment to the 30-keV transition and the $E1$ assignment for the one at 270 keV are consistent only with a spin and parity of $\frac{7}{2}^-$ or $\frac{9}{2}^-$ for the 270-keV state. But the character of the beta transition to this level rules out the possibility of $\frac{9}{2}^-$. (If the 240-keV state had $I^\pi=\frac{3}{2}^-$, the 270-keV level could have $I^\pi=\frac{3}{2}^-$, $\frac{5}{2}^-$, or $\frac{7}{2}^-$, although $\frac{7}{2}^-$ would be preferred since the $M1$ contribution to the 30-keV transition is small.)

The spin and parity assignment of the 114-keV level is limited to $\frac{5}{2}^+$ and $\frac{7}{2}^+$ by the logft of the beta transition to this state and the $M1$ character of the 114-keV transition. The fact that several neighboring nuclei have ground-state spins of $\frac{5}{2}$ would suggest some preference for $\frac{5}{2}^+$. By the same arguments, the 211-keV level should have a $\frac{5}{2}^+$ or $\frac{7}{2}^+$ assignment.

The beta branches to the states at 538, 654, and 768 keV imply that these levels have spin $\frac{3}{2}$, $\frac{5}{2}$, or $\frac{7}{2}$.[23a]

Comments

Although $_{61}Pm_{88}^{149}$ is in a region of mass which may be of theoretical interest, the lack of measurements of

[19] B. Burdick, W. M. Doyle, R. Marrus, and W. A. Nierenberg, Bull. Am. Phys. Soc. 7, 476 (1962).

[20] See, for example, M. G. Mayer and J. H. D. Jensen, in *Alpha-, Beta-, and Gamma-Ray Spectroscopy*, edited by Kai Siegbahn, (North-Holland Publishing Company, Amsterdam, 1965), Vol. 1, Chap. IV.

[21] B. R. Mottelson and S. G. Nilsson, Kgl. Danske Videnskab. Selskab, Mat. Fys. Medd. 1, No. 8 (1959).

[22] A. Y. Cabezas, I. Lindgren, and R. Marrus, Phys. Rev. 122, 1796 (1961).

[23] See, for example, I. Lindgren, in *Alpha-, Beta-, and Gamma-Ray Spectroscopy*, edited by Kai Siegbahn, (North-Holland Publishing Company, Amsterdam, 1965), Vol. 2, Appendix 4.

[23a] *Note added in proof.* Based on γ-γ angular correlation measurements, K. P. Gopinathan [Phys. Rev. 141, B1185 (1966)] reports spins for the levels at 114($\frac{5}{2}$), 210($\frac{5}{2}$,$\frac{7}{2}$), 272($\frac{7}{2}$,$\frac{5}{2}$), 538($\frac{5}{2}$), and 650 keV ($\frac{3}{2}$,$\frac{7}{2}$).

the spins of the various levels makes any detailed theoretical considerations of little interest. In addition to verification of the proposed decay scheme, studies of the gamma-gamma angular correlations would be of interest. Also more accurate measurements of the internal-conversion-electron intensities would help in determination of multipolarities and spins.

APPENDIX: DETERMINATION OF GAMMA-RAY INTENSITIES FROM SPECTRA FROM NaI(Tl) AND LITHIUM-DRIFTED GERMANIUM DETECTORS

In order to provide the reader with sufficient information to make a critical analysis of the gamma-ray intensities reported, a description of the methods used in the spectral analysis is presented.

About seventy gamma rays have been identified in the various experiments. It is clear that one cannot hope to determine the intensities of more than about a dozen transitions from the scintillation spectrum, Fig. 4, without the use of some other information. The internal-conversion studies and Ge detector spectra are, therefore, used to determine the number of transitions present, their energies, and some relative intensities. This information is then applied to the analysis of the spectrum obtained with the NaI spectrometer.

One might hope that it would be possible to determine the intensities from the spectra from a germanium detector. However, at present for resolved peaks, the intensity measurements with these detectors are probably not as accurate as those with a NaI(Tl) detector. For calculated photopeak efficiencies, this results in part from the lack of accurate knowledge of the sensitive volume of a detector. Also, the exclusive use of photoelectric cross sections for calculated efficiencies may be valid for only the smallest detectors since some Compton-scattering events may contribute to the photopeak. However, approximate relative intensities from the germanium detector data are useful for those gamma rays whose photopeaks are not resolved in the spectra from the NaI detector.

The photopeak efficiency for the germanium detectors was calculated and measured with respect to that for NaI detectors. For the computed efficiency, it was assumed that only the photoelectric process contributes. The photoelectric cross sections for germanium were interpolated from those in Ref. 24. The calculations were carried out in the same manner as those discussed in Ref. 25 for NaI(Tl) detectors. The results are shown in Fig. 12 for the detectors used. Calculations carried

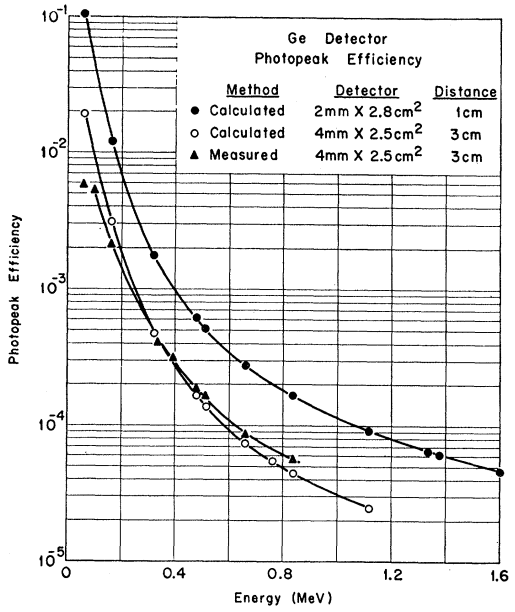

FIG. 12. Calculated and experimental photopeak efficiencies for germanium detectors of the sizes used. See text for discussion.

out for source-detector distances from 0.1 to 10 cm indicate that for distances from 1 to 4 cm the relative efficiencies between 0.1 and 1.3 MeV are the same within about 3%. Therefore, for relative intensity measurements, knowledge of the source distance and the constancy of this distance are not important. The peak efficiency was measured by comparing photopeak areas for spectra obtained from the NaI and germanium detectors, and correcting for the known NaI detector efficiency. These results, which include the absorption correction, are also shown in Fig. 12.

The relative gamma-ray intensities were determined from the Ge detector spectra in Figs. 2 and 3. This was done simply by adding up the counts in a photopeak, subtracting the estimated contribution from the underlying spectrum, and dividing by the photopeak efficiency. The results for these spectra are given in column 2 of Table XII. For transitions within 100 keV of each other, the calculated and experimental peak efficiencies give the same relative intensites to within ~5%. It is assumed that the relative intensities over such an energy range are accurate to ~5%. Over larger energy ranges the results of the analysis of the NaI detector spectrum are used.

In the analysis of the spectrum from the NaI(Tl) detector, Fig. 4, four types of information were used. These were the shape of the spectrum for each gamma ray, the shapes of the bremsstrahlung components, a computer program to do the analysis, and some of the relative intensities from Table XII. The component spectra for the gamma rays are computed by use of two programs which are described in Ref. 8. These programs carry out an interpolation between a set of

[24] C. M. Davisson, in *Alpha-, Beta-, and Gamma-Ray Spectroscopy*, edited by Kai Siegbahn (North-Holland Publishing Company, Amsterdam, 1965), Vol. 1, Appendix 1.

[25] S. H. Vegors, Jr., L. L. Marsden, and R. L. Heath, U. S. Atomic Energy Commission Report IDO-16370, 1958 (unpublished).

TABLE XII. Some results from the analysis of gamma-ray spectra. The components whose relative intensities were fixed are connected by a vertical line.

Transition energy (keV)	Ge(Li) detector: Data of Fig. 2 Experimental ϵ_p	Ge(Li) detector: Data of Fig. 3 Computed ϵ_p	Sample fits to NaI(Tl)-detector data: Fit No. 1	Fit No. 2	Fit No. 3	Fit No. 4
1456		0.0016	...	...		
1384		0.0015	...	...		
1359		0.0022	...	...		
~1336		<0.001	...	...		
1314		0.006	...	...		
1291		0.004	...	...		
1266		0.009	...	...		
1237		0.029	0.044±0.002	0.046±0.002		
1201		0.011	0.015	0.018		
1176		0.012	0.020	0.011		
1128		0.037	0.057±0.004	0.035±0.022		
1103		0.052	0.042	0.020		
1080		0.082	0.066±0.004	0.031±0.002		
1043		0.008	0.004	0.002		
1026		0.100	0.155±0.009	0.114±0.007		
980		0.079	0.154	0.062		
925		0.087	0.229±0.004	0.090±0.004		
~860		<0.05				
~840		<0.05	0.213±0.007	0.095±0.015		
~830		<0.05				
810		0.20	0.359±0.009	0.224±0.015		
~770		<0.07				
~755		<0.07	0.264±0.009	0.165±0.018		
712	0.08	0.07	0.143	0.051		
696	0.10	0.12	0.191	0.068		
686	0.06		0.101	0.035		
655	8.4		8.45 ±0.04	8.27 ±0.02		
631	0.2		0.31 ±0.02	0.106±0.018		
600	...	...	0.26 ±0.02	0.075±0.031		
581	0.15		0.125	0.18		
556	1.05		1.20 ±0.004	1.61 ±0.01		
541	6.3		6.91 ±0.02	6.25 ±0.07		
~490	...				0.24±0.07	0.13±0.02
~470	...				0.29±0.09	1.56±0.04
444	1.05				1.23	1.18
424	6.5				7.70±0.07	7.33±0.04
384	0.2				0.44	0.31
366	0.4				0.90±0.02	0.59±0.02
349	1.3				1.65	1.56
327	3.8				4.69±0.07	4.40±0.04
310	0.43				0.29	0.18
301	0.35				0.33±0.04	0.20±0.04
294	0.5				0.33	0.20
288	0.6					
283	0.4				2.93±0.22	2.93±0.22
275	0.5					
270	8.7				10.6 ±0.1	10.3 ±0.1
268	4.8				5.81	5.68
258	0.4				0.46	0.42
246	0.8				0.92	0.84
240	3.3				3.90±0.07	3.56±0.04
230	0.4				0.64	0.60
226	0.11					
214	~0.3					
211	22.2				27.6 ±0.1	27.5 ±0.1
208	2.5					
199	1.2				1.32	1.03
192	0.4				2.33±0.04	1.83±0.02
189	1.7					
178	0.2				...	...
156	5.6				5.94±0.07	5.46±0.04
139	0.5				0.59±0.04	0.02±0.02
127	0.13				...	...
122	0.22				...	...
114	19.2				19.1 ±0.1	18.4 ±0.1

TABLE XII (*continued*)

Transition energy (keV)	Ge(Li) detector: Data of Fig. 2 Experimental ϵ_p	Ge(Li) detector: Data fo Fig. 3 Computed ϵ_p	Sample fits to NaI(Tl)-detector data: Fit No. 1	Fit No. 2	Fit No. 3	Fit No. 4
97	1.6				1.39±0.04	···
74	2.6				1.98±0.07	···
59	1.3				1.58±0.07	···
1500-keV bremsstrahlung			0.18	1.5±0.2	···	···
1250-keV bremsstrahlung			0.09	0.0±2.0	···	···
channel range			105–250	105–250	13–100	24–100
Q			3.2	2.8	36	14
high-energy fit			···	···	No. 1	No. 2

experimental single gamma-ray shapes for the detector and gain scale of interest.

The computer program (SISYPHUS II) that was used to do the spectrum fitting can allow both the energies and the intensities of the components to vary. After the intensities are computed by a linear least-squares method, the energies are varied, one at a time, in finite increments which the user specifies. At each new position a new gamma-ray shape is computed. The program accepts any particular change in energy if it reduces the quantity $\sum_i w_i(y_i-\bar{y}_i)^2$. Here, y_i is the count in the ith channel of the experimental spectrum, $\bar{y}_i$ is the sum of the contributions of the components to this spectrum in channel i, w_i is a statistical weight, and the summation is over the desired range of channels. The fit is terminated when recalculation of the intensities and the energies does not reduce the quantity. The quality of fit is judged from the value of

$$Q=\frac{\sum w_i(y_i-\bar{y}_i)^2}{(n-m)},$$

where n is the number of channels in the summation and m is the number of variable intensities. Ideally, Q should be approximately unity for a satisfactory fit. However, larger values must be expected since the component shapes do not represent exactly the spectrum of the corresponding gamma ray. The program also computes error estimates for the intensities, but not for the energies. These estimates, however, are based on the assumption that the components are exact and, therefore, are not good estimates in all cases.

Besides the gamma-ray components, one needs shapes for the bremsstrahlung spectra. It was decided to approximate the bremsstrahlung from all of the beta-ray branches by two components. The five beta branches with intensities greater than 10% of decays range in energy from 1.0 to 1.55 MeV. The bremsstrahlung shape for Y^{91} ($E_{\beta^-}=1.55$ MeV) was measured, and, after subtraction of the 1.2-MeV gamma ray, used as one component. The second component, for an energy of about 1.1 MeV, was estimated by interpolation between a set of experimental bremsstrahlung shapes. All of these spectra were measured with sources whose disintegration rates had been determined by 4π β counting. From the decay scheme and the disintegration rates for these components and the Nd^{149} spectrum, it was determined that in the fit to the Nd^{149} spectrum the two bremsstrahlung components should be multiplied by approximately 0.18 and 0.09, respectively.

Because of limitations on data storage in the computer program, the Nd^{149} spectrum was analyzed in two sections. First, the gamma rays above 500 keV and the bremsstrahlung components were fitted. Second, those transitions below 500 keV were fitted to the spectrum obtained after subtracting the components in the first fit.

In fitting the high-energy portion of the spectrum, the bremsstrahlung components were handled in two different ways. First, their intensities were fixed at the above values of 0.18 and 0.09. The results of this fit are given in column 4 of Table XII. The intensities obtained when the bremsstrahlung intensities were allowed to vary are given in column 5. The quality of fit, as indicated by the value of Q, is better for the latter fit. The latter bremsstrahlung intensities differ drastically in relative intensity and by a factor of 5 in total intensity from the expected values. The reason for the program to prefer intensities other than the expected ones is not understood. In carrying out these fits, several relative intensities were fixed at the values determined from the germanium detector data. Also some of the energies were allowed to vary and some were not. Generally, the positions of the more intense gamma rays were allowed to vary and those of the weak ones were fixed. This is because the quality of the fit is often independent of the position of the latter transitions. The transitions whose energies were not well known (e.g., 480-keV doublet) were exceptions. They were allowed to have variable positions in spite of their weak intensity. The restrictions used are shown in the Table.

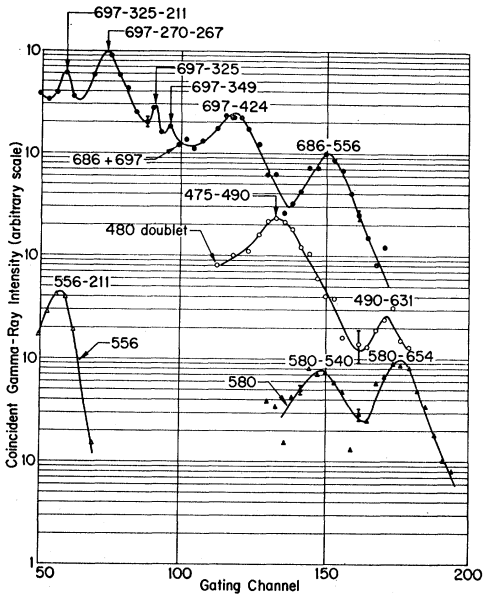

FIG. 13. Plots of the intensities of four gamma rays as a function of the gating channel in a gamma-gamma coincidence experiment. The peaks are labeled by the coincidence relation that is assumed to be responsible. A few typical errors, computed by the fitting program, are shown.

The errors quoted in the Table are from the computer program. For each group of related intensities the estimated error is given only for the most intense transition. The others have the same percentage error. It is pleasing to note that for the fit which has the lower Q, the intensities are in closer agreement with the intensities from the germanium detector data.

For these two fits to the high-energy region, the resulting components were subtracted from the original Nd^{149} data. These two resulting spectra were then fitted with the components below 500 keV. The results of two of these fits are given in Table XII. The poor quality-of-fit numbers (>10) are believed to be caused by the inability to generate shapes of below 150 keV of a quality comparable with statistical accuracy of the experimental data in this region. The intensities quoted in Table VI are based on these results together with the relative intensities over small energy intervals from the germanium detector data.

TABLE XIII. Quality of fits to gamma-gamma coincidence spectra.

Range of $\chi^2/(n-m)$	Number of fits
>3	4
2–3	9
1.5–2.0	7
1.0–1.5	24
<1.0	9

In order to determine coincidence relationships, sets of 256 gamma-gamma coincidence spectra were analyzed in a similar, but less exacting manner. For one set, all of the spectra with gates between 180 and 730 keV were fitted with about 20 gamma-ray components. The intensity of a component was then plotted as a function of the gating energy. The results for four components are shown in Fig. 13.

The quality Q of these fits is shown by the data in Table XIII. This range of values is considered to be satisfactory. Values greater than unity must be expected since the gamma-ray shapes used in the analysis are calculated for a different detector and for a geometry which yields a different spectrum of scattered radiation.

The delayed beta-gamma coincidence spectra that were used to determine the lifetime of the 240-keV level were also analyzed with SISYPHUS II. In this case the only components used were a 240-keV gamma-ray shape and the singles spectrum which represented the random coincidences.